Analysis of a Ship-to-Ship Collision*

V.L. Porter, D.J. Ammerman
Sandia National Laboratories

INTRODUCTION

Sandia National Laboratories is involved in a safety assessment for the shipment of radioactive material by sea. One part of this study is investigation of the consequences of ship-to-ship collisions. This paper describes two sets of finite element analyses performed to assess the structural response of a small freighter and the loading imparted to radioactive material (RAM) packages during several postulated collision scenarios with another ship. The first series of analyses was performed to evaluate the amount of penetration of the freighter hull by a striking ship of various masses and initial velocities. Although these analyses included a representation of a single RAM package, the package was not impacted during the collision so forces on the package could not be computed. Therefore, a second series of analyses incorporating a representation of a row of seven packages was performed to ensure direct package impact by the striking ship. Average forces on a package were evaluated for several initial velocities and masses of the striking ship. In addition to providing insight to ship and package response during a few postulated ship collisions scenarios, these analyses will be used to benchmark simpler ship collision models used in probabilistic risk assessment analyses.

PROBLEM DESCRIPTION

The problem modeled is that of a small freighter with the dimensions shown in Figure 1 impacted by ships of the same mass or more. The struck freighter is assumed to have a mass of 1675 metric tons and zero initial velocity. Two series of analyses were performed. In each series, the response of the freighter was evaluated when impacted by a striking ship of various masses travelling at various initial velocities normal to the longitudinal axis of the freighter. For all analyses the shape of the striking ship was the same as the shape of the struck freighter, with the exception that the bow of the striking ship was deeper than the bow of the freighter such that the striking ship strikes both the top deck and the bottom hull of the struck freighter. The striking bow was assumed to be vertical (zero rake angle), and

* This work was supported by the U. S. Department of Energy under Contract No. DE-AC04-94AL85000.

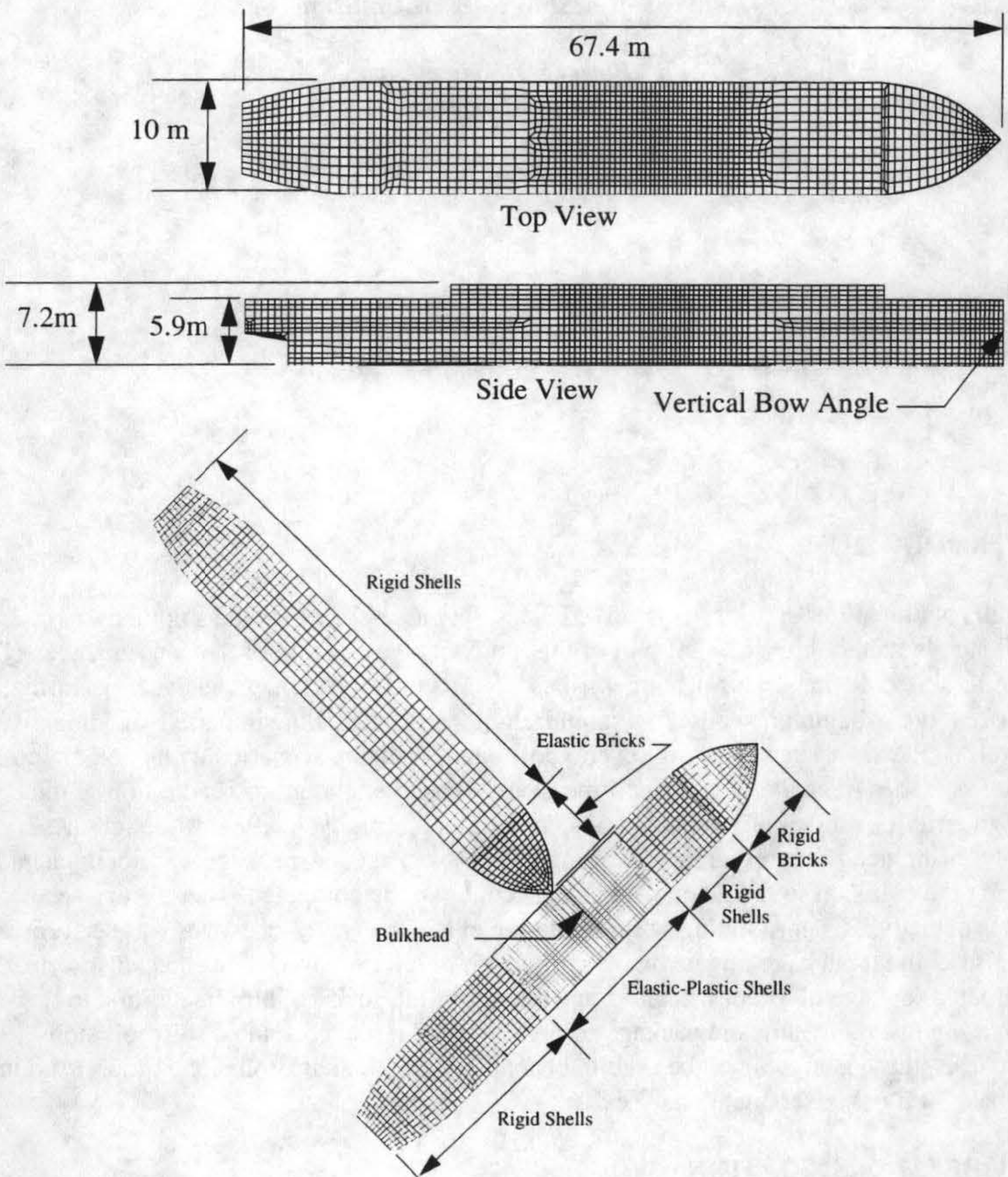

Figure 1. Finite element model.

all impacts were assumed to occur near the midsection of the freighter to maximize the damage incurred by the freighter. The first series of analyses (designated 1S to 4S) incorporated a crude representation of a single RAM package initially located adjacent to the hull of the freighter opposite the striking ship. The package represented is that of a 22.7 metric tons truck cask. In the second series (designated 1M to 4M), a representation of a row of similar packages was incorporated. Specific problem parameters are given in Table 1. Case 1 represents an accident that could take place in a harbor or other congested region, Case 2 is a representation of a real accident involving a small freighter. Cases 3 and 4 are upper bounds to the velocity that ships travel and an upper bound on the mass of a ship with this narrow of a bow. These cases were modeled to ensure analyses of severe damage were included.

Table 1: Problem Parameters

Case Designation	Initial Velocity of Striking Ship, knots (m/s)	Mass of Striking Ship, metric tons
1S, 1M	10 (5.14)	1675
2S, 2M	15 (7.73)	10,050
3S, 3M	25 (12.9)	16,750
4S, 4M	30 (15.6)	16,750

MODEL DESCRIPTION

In general, modeling the collision of two ships involves a very complicated coupled problem between the response of the water and the structural deformation of the ships. During a collision, kinetic energy is dissipated in structural deformation of the ships and by motion of water. However, review of previous published analyses which used a loosely coupled approach (Lenselink and Thung 1992), showed that the amount of kinetic energy that is dissipated in structural deformation is nearly the same whether or not the water is explicitly included in the analyses (Porter 1995). Therefore, in the analyses reported here, the water is not explicitly modeled. Rather, water effects are included following the method (Minorsky 1959) in which the mass of the struck ship is assumed to be 40% greater than its actual mass.

Most of the striking ship and the forward and aft portions of the struck ship are modeled using rigid elements. Because rigid elements are computationally efficient and do not influence the critical time step, their use allows a more refined mesh of deformable elements in the areas of importance, that is, in the areas of greatest deformation. The bow of the striking ship was modeled with eight-noded brick elements assumed to be elastic so that their deformation is negligible compared to the elastic-plastic shell elements in the midship section of the struck ship. This simulates a rigid bow so that nearly all deformation energy is incurred by the struck ship. The elements in the bow of the striking ship are modeled as elastic rather than rigid in order to allow the contact algorithm to properly distribute the contact forces.

The packages were modeled with a coarse mesh using elastic rectangular prisms with four elements each, because they were used only to evaluate average forces and not to analyze deformation. The multiple package representation consists of seven packages side-by-side spanning 80% of the breadth of the freighter. In order to get a conservative estimate of the forces on the packages, they were assumed to be rigidly tied together. In all analyses performed, the packages were free to move. No tie-downs were modeled, there was no gravity, and no friction.

In both series of analyses, the major components of the deformable part of the struck ship are the outer hull, a transverse bulkhead, a lower deck that extends the entire width of the ship, a partial middle deck, and the upper deck and hatch cover. The hatch cover was assumed to be rigidly attached to the upper deck to maximize the stiffness of the struck ship and its ability to impart load to the RAM packages. All elastic-plastic shell elements were thickened to represent the smeared effects of beams and stiffeners which could not practically be modeled explicitly with shell elements due to their small size. The thickened area of the shells was the same as the area of the hull with stiffeners. This approximation changes the local behavior of the shells and may have an affect on the initiation of tearing in the shells. All shell elements are four-noded quadrilaterals using five integration points through the thickness. These shells were assumed to be constructed of mild steel similar to ASTM A36.

Rigid elements were used to capture the proper geometry but were given a very small density. The motion of each block of rigid elements is controlled through the designation of a point mass at the desired center of gravity, in this case assumed to be near the center of each ship. Similarly, the rotational motion is controlled through the use of designated mass moments of inertia. To maximize deformation, the mass moments of inertia in each of the three global directions was set large enough to prevent large rotational motion.

RESULTS

As described above, a total of eight different ship collision scenarios were modeled. In each case, the Sandia-developed transient dynamics finite element code, PRONTO3D (Taylor and Flanagan 1989) was used running on a CRAY J90 machine. Run times averaged about 14 hours of CPU time for modeling one second of real time. However, the actual duration of impact as measured by time to maximum penetration turned out to be less than one second in all cases.

Finite element results of each scenario are described in detail below. The impact event was assumed to be over when maximum penetration was reached, or equivalently, when the kinetic energy reached a constant value, meaning that no additional energy was being dissipated by structural deformation.

Single Package Results

Results of the finite element computations for the first series of analyses with the single package representation are given in Table 2. Figures 2 and 3 contain plots of the deformation of the struck ship from three different views. In each case, two views from the top are shown, one including the top deck and hatch cover and a second in which these have been removed so that internal damage can be seen. A view of the internal damage and the package from the stern is also included. One can easily see the increased damage in case 4S. However, even in this case the striking ship only penetrated the struck ship to slightly

Table 2: Results Summary for Series S

Case	Impact Velocity (knots, m/s)	Initial Kinetic Energy (MJ)	Duration (s)	Loss in Kinetic Energy (MJ)	Maximum Penetration (m)	Velocity of Both Ships at Time of Max. Penetration (m/s)
1S	10, 5.14	22.1	0.27	11	0.8	2.0
2S	15, 7.73	300.3	0.50	95	2.2	5.8
3S	25, 12.9	1394	0.66	381	4.2	10.1
4S	30, 15.6	2038	0.68	493	5.2	12.5

more than half of its breadth. Therefore, during this series of analyses, the package initially located adjacent to the hull farthest from the striking ship was not directly impacted by the striking ship during the impact event.

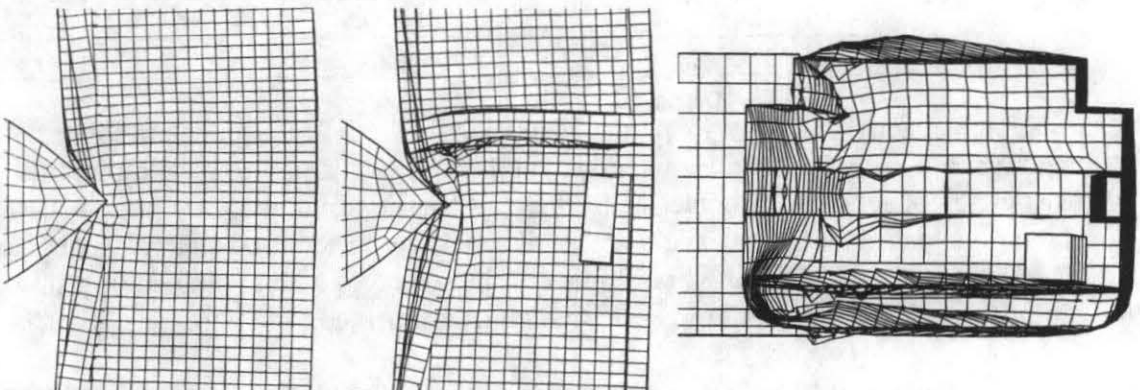

Top view with hatch cover in place. Top view without hatch cover and upper deck. View from stern.

Figure 2. Maximum deformation for Case 2S (v = 15 knots, mass = 10,050 tonnes, t = 0.50 seconds).

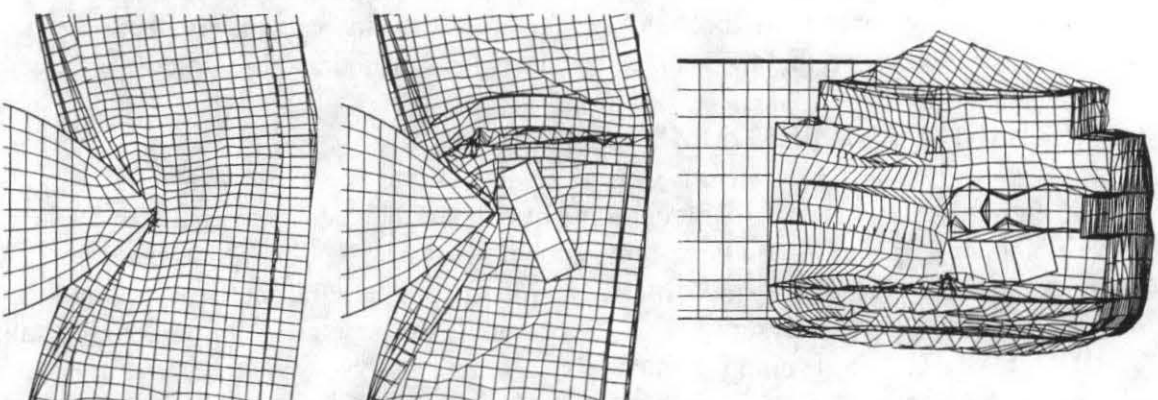

Top view with hatch cover in place. Top view without hatch cover and upper deck. View from stern.

Figure 3. Maximum deformation for Case 4S (v = 30 knots, mass = 16,750 tonnes, t = 0.68 seconds).

Multiple Package Results

A second series of analyses was conducted in order to measure the force that a RAM package might experience during a ship collision. In these analyses, a representation of a row of packages spanning 80% of the breadth of the ship was incorporated to ensure direct impact and crushing of the packages in at least some of the analyses. Table 3 summarizes the results for duration of impact and loss in kinetic energy for this series of analyses.

Table 3: Results Summary for Series M

Case	Duration (s)	Loss in Kinetic Energy (MJ)	Kinetic Energy of Striking Ship at Initial Impact with Packages (MJ)
1M	0.25	11	Did not impact.
2M	0.47	81	234
3M	0.58	356	1270
4M	0.50	369	1880

Deformation of the freighter at maximum penetration for Case 2M is shown in Figure 4. Although it is not clear from the views shown, at the time of maximum penetration the packages were not actually in contact with either side of the freighter hull. Figure 4 also shows the time history of the average force on the packages. The initial compressive peak at 0.27 seconds was caused by the first contact of the packages with the impending ship. Initial contact with the front hull forces the packages toward the back hull.

As shown in Figure 5, similar, but greater, deformation and loads are seen in Case 4M. Initial impact of the striking ship and forward hull on the packages occurs between 0.13 and 0.14 seconds, resulting in the initial peak compressive force of 370 MN. As in previous analyses, this is not a crushing force because the packages are not in contact with the back wall at this time. By 0.16 seconds, the packages have impacted the back hull, and at 0.22 seconds they are in contact with both sides of the hull simultaneously. By 0.30 seconds the packages have rotated so that the back end impacts the lower side of the middle decks.

CONCLUSIONS AND RECOMMENDATONS

Eight different scenarios of two ships colliding have been analyzed using transient dynamic finite element computations for three-dimensional structures. The first four analyses included a representation of a single truck cask initially placed adjacent to the hull opposite the striking ship. These analyses were used to compute the penetration of the striking ship into the hull of a common small freighter. None of these analyses resulted in the impact or crushing of the included package. The maximum penetration computed was 5.2 m, a distance only slightly greater than one-half of the breadth of the freighter. However, even with this amount of penetration, the hull of the struck ship indicated only minor tearing. Because the prediction of tearing is mesh dependent, more computations should be done with a finer mesh in the area of greatest plastic strain.

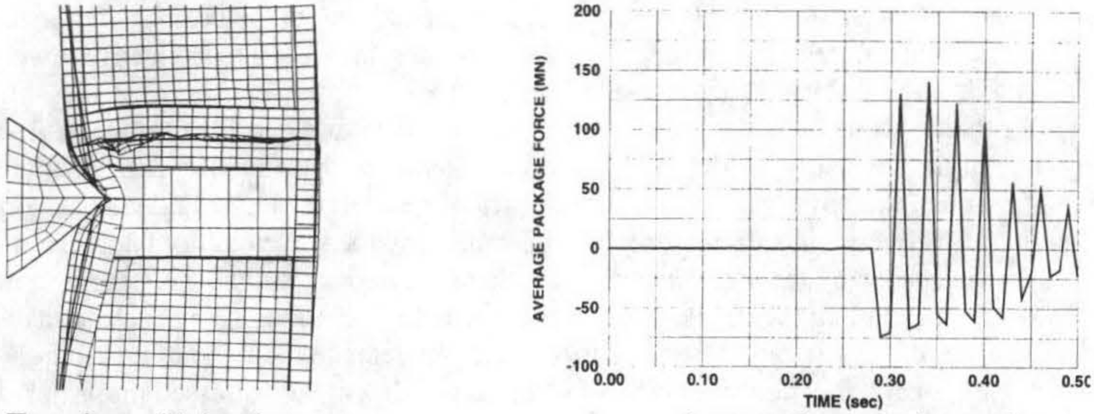

Top view with hatch cover and upper deck removed.

Average forces acting on the simulated RAM packages.

Figure 4. Maximum deformation and average force on the simulated radioactive material packages for Case 2M (v = 15 knots, mass = 10,050 tonnes, t = 0.47 seconds).

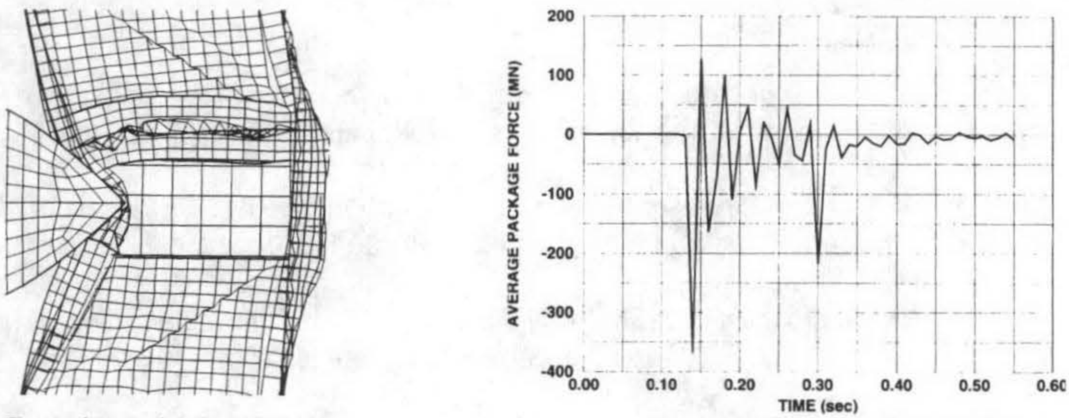

Top view with hatch cover and upper deck removed.

Average forces acting on the simulated RAM packages.

Figure 5. Maximum deformation and average force on the simulated radioactive material packages for Case 4M (v = 30 knots, mass = 16,750 tonnes, t = 0.50 seconds).

Each analysis in the second series included a representation of seven casks lying side-by-side spanning 80% of the breadth of the freighter to ensure impact and crushing of the packages in at least some of the analyses. Results show that the greatest force on the packages occurs at the initial impact with the forward side of the hull as the striking ship penetrates. Crushing forces that occur later during the collision are much less. These impact forces are likely less than would be seen during a regulatory drop test because the impact occurs at a lower velocity and the bow of the striking ship is not rigid.

The amount of penetration seen in these analyses is less than the amount predicted using simplified calculations, such as the Minorsky method, and the degree of tearing is less than is typically seen in this type of impact. Some of the reasons for these results are the fact the impact point on the struck ship is very near to the transverse bulkhead and partial between-decks. This is the stiffest region of the struck ship for side impacts. Also, the artificial stiffening of the shell elements to eliminate the need to model the beam stiffeners makes these elements more resistant to tearing. In all of these models the hatch covers were assumed to be rigidly attached to the top deck. This assumption causes the struck ship to be stiffer than it would be if the hatch covers were allowed to slip off the top deck. The final source of limited tearing is the mesh size. A coarser mesh distributes localized strains over a larger area, thereby reducing the average strain in the element and delaying the onset of tearing. It is likely the stiffening of the ship caused by these factors does not decrease the crush forces seen by the simulated radioactive material packages because these factors make the back hull of the struck ship stiffer as well. So even though the penetration distance and tearing of the forward portion of the ship are underestimated, the forces acting on the package are probably conservative. All of these issues will be addressed in further studies.

REFERENCES

Lenselink, H. and Thung, K.G. *Numerical Simulations of the Dutch-Japanese Full Scale Ship Collision Tests*, proceedings of the Conference on Prediction Methodology of Tanker Structural Failure (1992).

Porter, V. L. *Analysis of Water Effects during Ship Collisions as Modeled by Lenselink and Thung*, Sandia memo to D. J. Ammerman and M. B. Parks (1995).

Minorsky, V. U., *An Analysis of Ship Collisions with Reference to Protection of Nuclear Power Plants*, Journal of Ship Research, Vol. 3, No. 1 (1959).

Taylor, L. M., and Flanagan, D. P., *PRONTO-3D: A Three-Dimensional Transient Solid Dynamics Program*, SAND87-1912 (1989).